

## A BIOINFORMATICS ANALYSIS AND HOMOLOGY MODELING OF XYLANASE FROM *PSEUDOMONAS PUTIDA*

M. BAKLI <sup>1,2</sup>, Nouredine BOURAS <sup>3,4</sup>, R. PAȘCALĂU <sup>5</sup>, Laura ȘMULEAC <sup>5</sup>

<sup>1</sup> *Département de Biologie, Faculté des Sciences et Technologie, Université de Aïn Temouchent, B.P 284, 46000, Aïn Temouchent, Algeria.*

<sup>2</sup> *Physiologie, Physiopathologie et Biochimie de la Nutrition, Université de Tlemcen, Tlemcen, Algeria.*

<sup>3</sup> *Département de Biologie, Faculté des Sciences de la Nature et de la Vie et Sciences de la Terre, Université de Ghardaïa, Ghardaïa, Algeria.*

<sup>4</sup> *Laboratoire de Biologie des Systèmes Microbiens (LBSM), Ecole Normale Supérieure de Kouba, Alger, Algeria.*

<sup>5</sup> *Banat's University of Agriculture Science and Veterinary Medicine "King Michael I of Romania", Faculty of Agriculture, 119 Calea Aradului, 300645, Timisoara, Romania.*

Corresponding author: mahfoud.bakli@gmail.com

**Abstract.** Xylanases (EC 3.2.1.x) are a widespread group of hydrolytic enzymes involved in xylan depolymerization. Xylan, the second most abundant polysaccharide in nature, is the major hemicellulosic constituent of the plant cell wall. To date, due to their eco-friendly nature xylanase, individually or in combination with other enzymes, have a widespread uses in various sectors of industries and agri-food processes. Xylanases are mainly produced by several microorganisms including bacteria, micro-fungi, algae, and some yeast. However, bacterial xylanases have been shown to possess an easy downstream process of industrial production with high production rate, and to ensure a more cost-effective process. Despite several reports investigating characterization, production, optimization, and isolation of xylanases from different *Pseudomonas* species, a study on the xylanase of the *P. putida* is still lacking. Recently, *P. putida* has emerged as a promising bacterial host for industry and plant biomass valorization due to its remarkably versatile metabolism, unique capacity to adapt to harsh environmental conditions, and to resist to difficult redox reactions, industrial solvents, and oxidative stresses. The aim of this study was to characterize xylanase from *P. putida* using bioinformatics analyses and homology modeling method. The secondary structural features of the protein was calculated by both PSIPRED and SOPMA tools which revealed that xylanase protein is composed of  $\alpha$ -helix (41.74%), random coils (34.86 %), extended strand (16.60 %), and  $\beta$ -turn (7.80 %). The three-dimensional structure of xylanase protein model was predicted by homology modeling through the Phyre<sup>2</sup> server. The structural refinement of this builded model was generated using Modrefiner and validated through the Ramachandran plot as obtained using the PROCHECK tool. Ligand binding site prediction by COFACTOR server was confident with a BS-score > 0.5. Protein-protein interaction networks demonstrated that xylanase had ten potential interacting partners with a high confidence score. The outcome of this *in silico* analysis could help for detection and characterization of such enzyme allowing its wide production and exploiting in various industrial and agri-food sectors.

**Keywords :** Xylanase, *Pseudomonas putida*, *in silico* analysis, homology modeling.

### INTRODUCTION

Xylan is the most abundant type of hemicelluloses in nature which is a principal structural component in plant cell walls and accounts for a large part of plants biomass. It is a polysaccharide composed by a linear backbone of  $\beta$ -1,4-linked xylose units (Talens-Perales et al., 2020). Xylan can be depolymerized using xylanase enzymes, an important family of hydrolases (Ariaeenejad et al., 2018). In recent years, due to their eco-friendly nature xylanases

(EC 3.2.1.x) individually or in combination with other enzymes, have aroused an ever-increasing interest due to the growing demand in industries and agri-food sectors (Chakdar et al., 2016). Therefore, these enzymes have found important applications in manufacturing of animal feed, plant biomass saccharification, production of xylitol as a natural sweetener, fruit juice clarification, enhancing of baked goods quality, textile, pulp and paper biobleaching, agricultural waste treatment and valorization, biotechnology, and bioethanol production (Basit et al., 2020; Vasić et al., 2021). Wide range of microorganisms such as bacteria, fungi, yeast, and some algae are used extensively for xylanase production (Bhardwaj et al., 2019). However, bacteria have an advantage over fungi for xylanase production because of neutral or alkaline pH range compared to that of fungal xylanases which is acidic (Chakdar et al., 2016). In addition, bacterial xylanases possess an easy downstream process of industrial production with high production rate, and to ensure a more cost-effective process (Dutta et al., 2018). Moreover, a variety of agro-byproducts including wheat bran, rice bran, rice straw, sugarcane bagasse, sawdust, and wheat husk could give a high-efficiency in xylanase production via microbial fermentation (Tran et al., 2021). Despite several reports investigating characterization, production, optimization, and isolation of xylanases from different *Pseudomonas* species including *P. cellulose* (Emami et al., 2002), *P. mohnii* (Paul et al., 2020), *P. boreopolis* (Guo et al., 2018), *P. nitroreducens* (Dhivahar et al., 2020), while a study on xylanase of the *P. putida* species is still lacking. Recently, *Pseudomonas putida* has been considered as promising host organism for plant biomass valorization (Elmore et al., 2020) due to its outstanding properties to adapt to harsh environmental conditions, especially high concentrations of organic solvents, difficult redox reactions, and oxidative stresses (Martin-Pascual et al., 2021). Additionally, *Pseudomonas putida* is a well-characterized Gram-negative soil bacterium endowed with many attractive traits such as its simple nutritional requirements, fast growth, and flexible metabolism that make it a suitable chassis for contemporary, industrially oriented metabolic engineering (Löwe et al., 2017; Martin-Pascual et al., 2021). Furthermore, this bacterium is also suitable for other agricultural applications including plant-growth promoting properties and phytopathogen biocontrol activity (Bakli and Zenasni, 2019).

Indeed, detailed understanding characteristics of xylanase proteins can be achieved through their amino acid sequences and 3D structures. Moreover, identification of the tertiary structure of a protein including X-ray crystallography or nuclear magnetic resonance techniques (NMR) are time-consuming, expensive, and not successful with all proteins (Bakli et al., 2020). However, the *in silico* homology modeling provides an alternative application to predict the 3D protein structure with better validation (Karunarathna et al., 2020). The present study aimed at *in silico* approach and homology modeling of xylanase protein from *P. putida* to elucidate the physicochemical properties, predicted structure of the protein as well as the functional analysis.

## MATERIALS AND METHODS

### 1. Protein sequence recovery

The amino acid sequence of xylanase from *Pseudomonas putida* DLL-E4 strain was retrieved in FASTA format from the National Center for Biotechnology Information database, (NCBI) (<http://www.ncbi.nlm.nih.gov>) (Coordinators, 2018) with the GenBank accession ID of AHZ76548.1 and served as query sequence for all bioinformatics analyses. The same FASTA sequence was used as a query sequence for the PSI-BLAST (Position-Specific Iterative Basic

Local Alignment Search Tool) against protein data bank (PDB) at (<http://blast.ncbi.nlm.nih.gov/Blast.cgi>) to identify its homologous structures.

## **2. Analysis of physicochemical properties**

The primary sequence analysis for the *P. putida* xylanase protein was executed by determining the computation of various physical and chemical parameters from ExPASy ProtParam tool (<http://expasy.org/tools/protparam.html>) (Gasteiger et al., 2005). This server tool analyses length of sequence, amino acid composition, molecular weight (MW), theoretical isoelectric point (pI), aliphatic index (AI), instability index (II), number of positive and negative charged residues (R+/-), extinction coefficient (EC), estimated half-life, and grand average of hydrophobicity (GRAVY).

## **3. Subcellular localization, solubility prediction, and peptide signal prediction**

The subcellular localization of the xylanase protein was predicted by CELLO 2.5 server (<http://cello.life.nctu.edu.tw/>) (Yu et al., 2006). Moreover, solubility prediction was carried out using the SOSUI server (<http://harrier.nagahama-i-bio.ac.jp/sosui/>) (Hirokawa et al., 1998) in order to identify the transmembrane helices in the xylanase protein. Signal peptide prediction was performed using SignalP-5.0 server (<http://www.cbs.dtu.dk/services/SignalP/>) (Armenteros et al., 2019).

## **4. Secondary structure analysis**

Both PSI-BLAST-based secondary structure PREDiction, PSIPRED 4.0 (<http://bioinf.cs.ucl.ac.uk/psipred/>) tool (McGuffin et al., 2000) and Self-Optimized Prediction Method with Alignment (SOPMA) tool (Geourjon and Deleage, 1995) from the Network Protein Sequence Analysis (NPS@) server ([https://npsa-prabi.ibcp.fr/cgi-bin/npsa\\_automat.pl?page=/NPSA/npsa\\_sopma.html](https://npsa-prabi.ibcp.fr/cgi-bin/npsa_automat.pl?page=/NPSA/npsa_sopma.html)) were employed to predict the arrangement of secondary structure elements including  $\alpha$ -helices,  $\beta$ -turn, extended strand,  $\beta$ -sheet, and coils of the retrieved xylanase amino acid sequence from *P. putida*.

## **5. Tertiary structure analysis, refinement, and validation**

The tertiary structure of the xylanase from *P. putida* protein was constructed by using the Protein Homology/analogy Recognition Engine server V2.0, Phyre<sup>2</sup> (<http://www.sbg.bio.ic.ac.uk/~phyre2/html/page.cgi?id=index>) (Kelley et al., 2015), which provides high quality structural model by using the template of primary protein sequence. Whereas, the predicted structural model was further refined using ModRefiner (<http://zhanglab.cmb.med.umich.edu/ModRefiner/>) server (Xu and Zhang, 2011). Then, the refined structural model so obtained was validated by quantifying the amino acid residues present in the Ramachandran plot. The stereochemical quality of the xylanase protein model was analyzed by PROCHECK tool (Laskowski et al., 1993) in structural analysis and verification server, SAVES v6.0 (<http://nihserver.mbi.ucla.edu/SAVES/>). The protein model was visualized and optimized by using PyMOL Molecular Graphics System software, Version 2.3 (DeLano, 2019).

## **6. Functional analysis**

In order to investigate the interaction of xylanase protein of *P. putida* with other closely related proteins STRING v11.5 (<http://string-db.org/>) server was utilized (Szklarczyk et al., 2021). This server is used to construct a protein-protein interaction network for different known and predicted protein interactions. Moreover, MOTIF finder online library (<http://www.genome.jp/tools/motif/>) was carried out to analyse common functional motifs and determine the family which the xylanase protein belongs. Additionally, the prediction of ligand

binding site (active site) of the xylanase enzyme from *P. putida* was performed by using COFACTOR server (<http://zhanglab.ccmb.med.umich.edu/COFACTOR/>) (Roy et al., 2012) based on structure of generated model, sequence, and protein–protein interaction.

## RESULTS AND DISCUSSIONS

### 1. Primary structural analysis

After amino acid sequence retrieval of xylanase from *P. putida*, its physicochemical properties (**Table 1**) was assessed using ExPASy ProtParam tool. The xylanase protein consists of 218 amino acid residues with a molecular weight of 24892.42 Da. The theoretical isoelectric point (pI) of this protein was 3.58 which suggest that the xylanase protein is extremely acidic, containing a total number of 26 negatively charged residues (Asp + Glu), and the total number of positively charged residues (Arg + Lys) is 24. The instability index (II) was 52.69 (> 40) which classified the xylanase as highly unstable protein.

The aliphatic index (AI) of a protein is defined as the relative volume occupied by its aliphatic side chains (alanine, valine, isoleucine, and leucine). AI value was found to be 86.88, indicating that the xylanase protein is thermostable over a wide temperature range (Ikai, 1980). The GRAVY (the Grand average of hydropathicity) score is calculated as the sum of hydropathy values of all amino acids in the protein, divided by the number of residues in the protein (Kyte and Doolittle, 1982). It represents the protein-water interactions.

The GRAVY value was found to be negative, indicating the hydrophilic nature of the xylanase enzyme. This information might be useful for localizing these proteins.

Table 1

Physicochemical properties of the xylanase from *P. putida*.

Property	Value
Number of amino acids residues (AA)	218
Molecular weight	24892.42
Theoretical pI	3.58
Total number of negatively charged residues (Asp)	26
Total number of positively charged residues (Arg)	24
Extinction coefficient (EC)	52160
half-life	30 hours
Instability index (II)	52.69
Aliphatic index (AI)	86.88
Grand average of hydropathicity (GRAVY)	-0.261

A BLASTp search against Protein Data Bank (PDB) was carried out, to find the most suitable protein structures as templates for the xylanase protein sequence of *P. putida*.

The result of the BLASTp is displayed in **Table 2**, which shows five resulting hits including PDB structural codes (accession number). The query coverage is higher ranged from 99% to 97%, and the percentage of identity ranged from 56.36 to 25 %.

Table 2

Hits of BLASTp on the xylanase sequence against Protein Data Bank (PDB)

No.	Accession number	Max score	Total score	Query coverage	E value	Per. ident	Accession length	Resolution(Å)	Description	Organism
1	1Z7A	255	255	99%	4e-85	56.36%	308	1.71	probable polysaccharide deacetylase	<i>Pseudomonas aeruginosa</i> PAO1
2	3CL6	255	255	99%	4e-85	55.91%	308	2.25	Puue Allantoinase	<i>Pseudomonas fluorescens</i>
3	3S6O	241	241	99%	2e-79	52.91%	321	1.85	polysaccharide deacetylase family protein	<i>Burkholderia pseudomalle</i>
4	3RXZ	75.9	75.9	97%	7e-16	31.67%	300	2.01	putative polysaccharide deacetylase	<i>Mycobacterium smegmatis</i>
5	3QBU	72.0	72.0	98%	2e-14	25.00%	326	2.2	putative peptidoglycan deactelyase (HP0310)	<i>Helicobacter pylori</i>

Subcellular localization prediction by CELLO program indicated that xylanase protein from *P. putida* was cytoplasmic with the highest reliability of 0.964. Furthermore, solubility prediction was conducted using SOSUI server which calculates average hydrophobicity and determines whether the protein is soluble or transmembrane protein. Thus, any hydrophobic portion in the protein is labeled as transmembrane region. SOSUI predicted the xylanase sequence as non transmembrane soluble protein. SignalP server suggested no signal peptide in this protein.

## 2. Secondary structure prediction

According to Self-Optimized Prediction Method with Alignment (SOPMA) tool by using its default parameters (window width, 17; similarity threshold, 8; and number of states, 4),  $\alpha$ -helix was found to be the most predominant (41.74%) one followed by the random coil (34.86%), extended strand (16.60%), and  $\beta$ -turn (7.80%).

Secondary structure of the xylanase protein of *P. putida* was also predicted by the PSI-BLAST-based secondary structure PREDiction, PSIPRED 4.0 server. The PSIPRED secondary structure prediction result seems to be in agreement with SOPMA result and had a high confidence of prediction (**Figure1**).

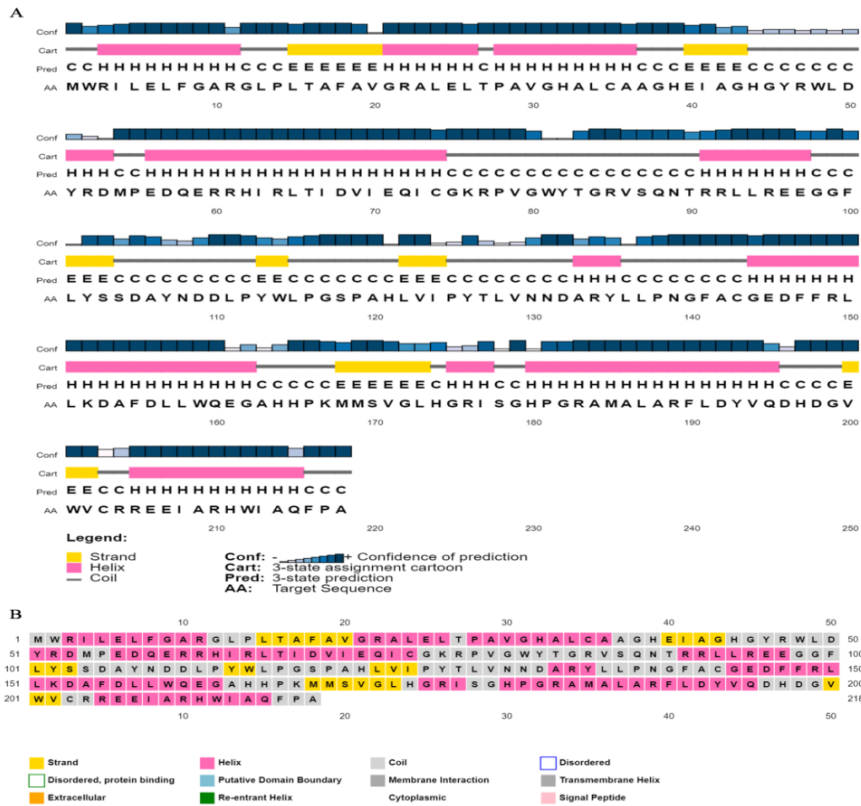


Fig. 1. Secondary structure prediction of *P. putida* xylanase by PSIPRED 4.0 server. (A) Graphical representation. (B) Sequence annotation plot. The colors represent protein secondary structure elements (yellow for  $\beta$ -strands, pink for  $\alpha$ -helix and grey for coil structures). The confidence of prediction observed throughout the predicted secondary structure was high, indicating high reliability of this prediction.

### 3. Tertiary structure analysis, refinement, and validation

The three-dimensional structure of *P. putida* xylanase was not available as yet at PDB. Therefore, the Protein Homology/analogy Recognition Engine server V2.0, Phyre<sup>2</sup> software results indicated that the secondary structure of xylanase showed identity 56%, 218 residues (100% of the xylanase protein sequence coverage) have been modeled with 100.0% confidence by the single highest scoring template, the crystal structure of probable polysaccharide deacetylase from *Pseudomonas aeruginosa* PAO1 (pdb, d1z7aa1). This template belongs to Glycoside hydrolase/deacetylase superfamily with 7-stranded beta/alpha barrel protein fold. The 3-D structure of the xylanase was successfully analyzed by Phyre<sup>2</sup> tool and visualized by PyMOL (Figure 2).



Fig. 2. Predicted 3D structure of xylanase from *P. putida* produced by Phyre<sup>2</sup>, refined by ModRefiner server and visualized by PyMOL 2.3 molecular graphics software. Secondary structure prediction of xylanase showing  $\alpha$ -helix (orange),  $\beta$ -sheets (yellow), and loops (cyan).

This result confirmed the most suitable protein structures as templates (first hit) found by BLASTp on the xylanase sequence against the Protein Data Bank, PDB (See above, table 2). Furthermore, the most accurate computational method to generate reliable structural models of proteins was homology modeling method and it was used in many biological applications. Model quality assessment tools were used to estimate the reliability of the models (Bordoli et al., 2009). In addition, the stereochemical quality of the predicted model and accuracy of the protein model was evaluated after the refinement process using Ramachandran map calculations computed with the PROCHECK program in the structural analysis and verification server, SAVES v6.0 (Bakli et al., 2021). The assessment of the xylanase predicted model generated by Phyre<sup>2</sup> server was shown in **Figure 3**.

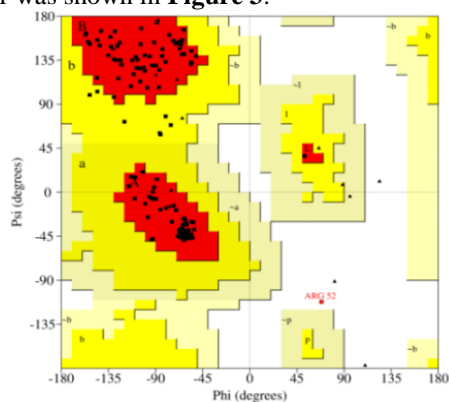


Fig. 3. Structure validation by Ramachandran plot of the *P. putida* xylanase model from PROCHECK (SAVE v6.0 server). The most favored regions are marked as A, B, and L (red). The additional allowed regions are marked as a, b, l, and p (yellow), generously allowed regions are marked as ~a, ~b, ~l, and ~p (light yellow) and disallowed regions (white). All non-glycine and non-proline residues are shown as filled black squares, while glycines (non-end) are shown as filled black triangles.

Ramachandran plot statistics of xylanase model displayed that 175 amino acid residues (95.6%) are in the favored region [A, B, and L], 7 amino acid residues (3.8%) are in the additional allowed region [a, b, l, and p], and no amino acid residue (0.0%) was in the

generously allowed region [~a, ~b, ~l, and ~p], while only one amino acid residues (0.5%) was in the disallowed region in xylanase protein. Hence, Ramachandran plot of the xylanase validate the refined 3D model structure of xylanase, because of this model is following dihedral angles of Ramachandran plot occupied favorable positions.

#### 4. Functional analysis

Xylanase protein from *P. putida* was selected as query sequence, and functional protein association network was generated using the STRING (Search Tool for the Retrieval of Interacting Genes/Proteins) v 11.5 database. This database is a biological database used to construct a protein–protein interaction network for different known and predicted protein interactions (Szklarczyk et al., 2021). Accordingly, functional analysis as resolved by STRING analysis detected ten potential interacting partners of xylanase protein (node, AGN79914.1) from *P. putida* in the protein interaction network with high confidence scores ranging from 0.991 to 0.788. Therefore, the closest interacting protein was detected with the shortest node, AGN79915.1 (OHCU decarboxylase) and having a score of 0.991 while the distant interacting protein was detected with the distant node, AGN79911.1 (GntR family transcriptional regulator) and having a score of 0.788. Protein-protein interaction of *P. putida* xylanase generated through STRING is presented in **Figure 4 and Table 3**.

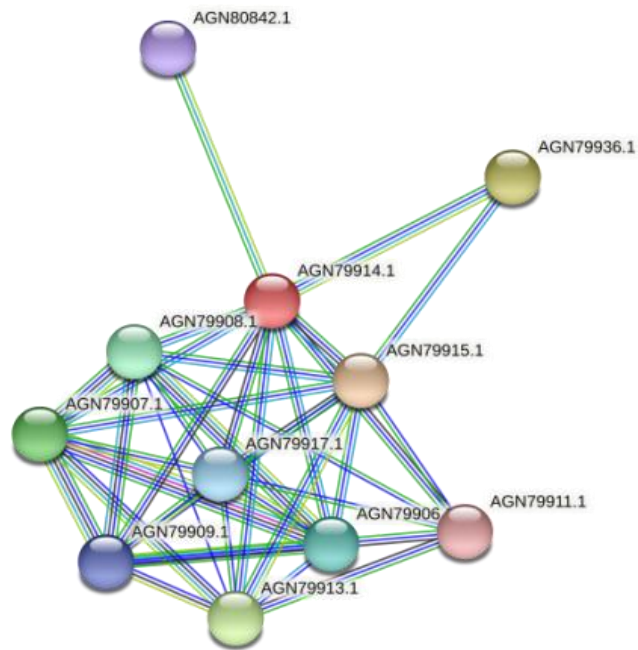


Fig. 4. Protein–protein interaction network analysis for the *P. putida* xylanase detected through STRING database. The red node (xylanase from *P. putida*) and other nodes represented its predicted functional partners from *P. putida* (Table 3).

Predicted functional protein partners of *P. putida* xylanase

Node	Annotation
AGN79915.1	OHCU decarboxylase
AGN79936.1	Asp/Glu/hydantoin racemase
AGN79913.1	5-hydroxyisourate hydrolase
AGN79907.1	Xanthine dehydrogenase
AGN79908.1	Molybdenum cofactor sulfurylase
AGN79906.1	Molybdopterin dehydrogenase
AGN79917.1	Membrane protein
AGN79909.1	Guanine deaminase
AGN79942.1	Transketolase
AGN79911.1	GntR family transcriptional regulator

Besides, COFACTOR software identified important active site amino acid residues involved in ligand binding site of the modeled *P. putida* xylanase, which are as follow: histidine 44, tryptophan 48, tyrosine 82, threonine 83, glycine 84, arginine 85, alanine 133, and histidine 174. BS-score, a measure of local similarity (sequence & structure) between template binding site and predicted binding site in the query structure was 1.15 ( $> 0.5$ ). It represents a significant local match between the predicted and template binding site (**Figure 5**). In this case, the best protein template with similar binding site was puue allantoinase complexed with 5-aminoimidazole-4-carboxamide (ligand) from *Pseudomonas fluorescens*, pdb id, 3CL8.

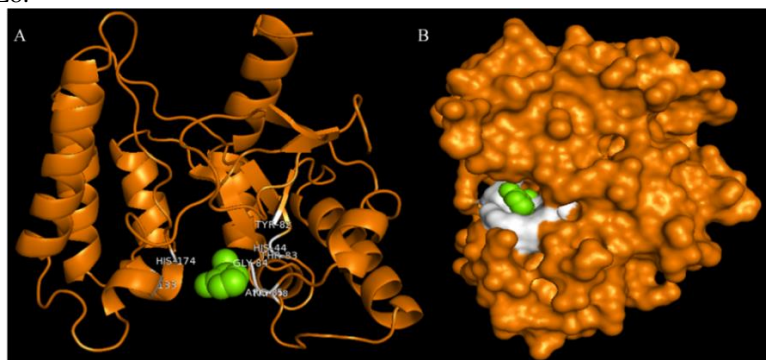


Fig. 5. Ligand binding sites of xylanase from *P. putida* predicted by COFACTOR and visualized by PyMOL 2.3 molecular graphics software. (A) Showing ligand binding sites (His 44, Trp 48, Tyr 82, Thr 82, Gly 84, Arg 85, Ala 133, and Ala 174). (B) Surface view of the xylanase protein with ligand in pocket exposed active site. Spheres represent the ligand (green). Ligand binding sites (white) with in xylanase structure (orange).

From the functional study of *P. putida* xylanase, MOTIF finder server detected one functional motif, polysaccharide deacetylase (NCBI Accession No. PF01522 in PFam database) at 2-95 position with an E-value of  $3.6e-12$  (**Figure 6**).

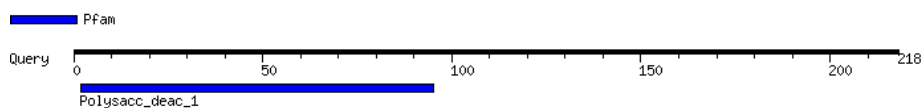


Fig. 6. MOTIF finder result showing functional motif for the *P. putida* xylanase.

Polysaccharide deacetylases (PDAs) belong to the carbohydrate esterase family 4 (CE4) in the Carbohydrate-Active Enzyme (CAZY) database (<http://www.cazy.org/>) (Terrapon et al., 2017). In this case, PDAs catalyse the hydrolysis of *O*-linked acetyl groups from *O*-acetylxylose residues (acetylxylosterases, xylanases) through a conserved catalytic core, termed the NodB homology domain (Andreou et al., 2018). Moreover, it has been shown that some long bacterial xylanases displayed an extra catalytic domain for polysaccharide deacetylase (Talamantes et al., 2016).

Both physicochemical characteristics (thermostability) and secondary structure properties of *P. putida* xylanase highlighted in our study were in concordance with an *in silico* study of 36 different xylanases from other bacterial origin (Dutta et al., 2018).

In sum, more structural, evolutionary, and functional studies are required to better understand the structure-function relations of this bacterial xylanase enzyme.

## CONCLUSIONS

In order to fulfill to the high demand in both industrial and agri-food sectors for the enzyme xylanase, there is a need in the future to produce more enzymes on a large scale. The present study should provide structural insights on bioinformatics study to determine the characteristics of xylanase enzyme in terms of its physicochemical and structural properties from a promising bacterial host for industry and plant biomass valorization bacterial host, *Pseudomonas putida*.

## BIBLIOGRAPHY

- ANDREOU, A., GIASTAS, P., CHRISTOFORIDES, E., AND ELIOPOULOS, E.E. (2018). Structural and evolutionary insights within the polysaccharide deacetylase gene family of *Bacillus anthracis* and *Bacillus cereus*. *Genes* 9, 386.
- ARIAEENEJAD, S., MOUSIVAND, M., MORADI DEZFOULI, P., HASHEMI, M., KAVOUSI, K., AND HOSSEINI SALEKDEH, G. (2018). A computational method for prediction of xylanase enzymes activity in strains of *Bacillus subtilis* based on pseudo amino acid composition features. *PLoS One* 13, e0205796.
- ARMENTEROS, J.A., TSIRIGOS, K.D., SØNDERBY, C.K., PETERSEN, T.N., WINTHER, O., BRUNAK, S., VON HEIJNE, G., AND NIELSEN, H. (2019). SignalP 5.0 improves signal peptide predictions using deep neural networks. *Nat Biotechnol* 37, 420-423.
- BAKLI, M., BOURAS, N., PAŞCALĂU, R., AND ŞMULEAC, L. (2021). *In silico* characterization of a cutinase from *Pseudomonas fluorescens*. *Research Journal of Agricultural Science* 53.
- BAKLI, M., KARIM, L., MOKHTARI-SOULIMANE, N., MERZOUK, H., AND VINCENT, F. (2020). Biochemical characterization of a glycosyltransferase Gtf3 from *Mycobacterium smegmatis*: a case study of improved protein solubilization. *3 Biotech* 10, 1-13.
- BAKLI, M., AND ZENASNI, A. (2019). Isolation of fluorescent *Pseudomonas* spp. strains from rhizosphere agricultural soils and assessment of their role in plant growth and phytopathogen biocontrol. *Research Journal of Agricultural Science* 51, 20-29.
- BASIT, A., JIANG, W., AND RAHIM, K. (2020). Xylanase and its industrial applications. In *Biotechnological Applications of Biomass* (IntechOpen).

- BHARDWAJ, N., KUMAR, B., AND VERMA, P. (2019). A detailed overview of xylanases: an emerging biomolecule for current and future prospective. *Bioresources and Bioprocessing* 6, 1-36.
- BORDOLI, L., KIEFER, F., ARNOLD, K., BENKERT, P., BATTEY, J., AND SCHWEDE, T. (2009). Protein structure homology modeling using SWISS-MODEL workspace. *Nature protocols* 4, 1-13.
- CHAKDAR, H., KUMAR, M., PANDIYAN, K., SINGH, A., NANJAPPAN, K., KASHYAP, P.L., AND SRIVASTAVA, A.K. (2016). Bacterial xylanases: biology to biotechnology. *3 Biotech* 6, 1-15.
- Coordinators, N.R. (2018). Database resources of the national center for biotechnology information. *Nucleic acids research* 46, D8.
- DELANO, W. (2019). The PyMOL Molecular Graphics System, version 2.3. 1. Schrodinger LLC: New York, NY, USA.
- DHIVAHAR, J., KHUSRO, A., PARAY, B.A., REHMAN, M.U., AND AGASTIAN, P. (2020). Production and partial purification of extracellular xylanase from *Pseudomonas nitroreducens* using frugivorous bat (*Pteropus giganteus*) faeces as ideal substrate and its role in poultry feed digestion. *Journal of King Saud University-Science* 32, 2474-2479.
- DUTTA, B., BANERJEE, A., CHAKRABORTY, P., AND BANDOPADHYAY, R. (2018). *In silico* studies on bacterial xylanase enzyme: Structural and functional insight. *Journal of Genetic Engineering and Biotechnology* 16, 749-756.
- ELMORE, J.R., DEXTER, G.N., SALVACHÚA, D., O'BRIEN, M., KLINGEMAN, D.M., GORDAY, K., MICHENER, J.K., PETERSON, D.J., BECKHAM, G.T., AND GUSS, A.M. (2020). Engineered *Pseudomonas putida* simultaneously catabolizes five major components of corn stover lignocellulose: Glucose, xylose, arabinose, p-coumaric acid, and acetic acid. *Metabolic Engineering* 62, 62-71.
- EMAMI, K., NAGY, T., FONTES, C.M., FERREIRA, L.M., AND GILBERT, H.J. (2002). Evidence for temporal regulation of the two *Pseudomonas cellulosa* xylanases belonging to glycoside hydrolase family 11. *Journal of bacteriology* 184, 4124-4133.
- GASTEIGER, E., HOOGLAND, C., GATTIKER, A., WILKINS, M.R., APPEL, R.D., AND BAIROCH, A. (2005). Protein identification and analysis tools on the ExPASy server. *The proteomics protocols handbook*, 571-607.
- GEOURJON, C., AND DELEAGE, G. (1995). SOPMA: significant improvements in protein secondary structure prediction by consensus prediction from multiple alignments. *Bioinformatics* 11, 681-684.
- GUO, H., HONG, C., ZHENG, B., JIANG, D., AND QIN, W. (2018). Improving enzymatic digestibility of wheat straw pretreated by a cellulase-free xylanase-secreting *Pseudomonas boreopolis* G22 with simultaneous production of bioflocculants. *Biotechnology for biofuels* 11, 1-10.
- HIROKAWA, T., BOON-CHIENG, S., AND MITAKU, S. (1998). SOSUI: classification and secondary structure prediction system for membrane proteins. *Bioinformatics (Oxford, England)* 14, 378-379.
- IKAI, A. (1980). Thermostability and aliphatic index of globular proteins. *The Journal of Biochemistry* 88, 1895-1898.
- KARUNARATHNA, K., SENATHILAKE, N., MEWAN, K., WEERASENA, O., AND PERERA, S. (2020). *In silico* structural homology modeling of EST073 motif coding protein of tea *Camellia sinensis* (L). *Journal of Genetic Engineering and Biotechnology* 18, 1-10.
- KELLEY, L.A., MEZULIS, S., YATES, C.M., WASS, M.N., AND STERNBERG, M.J. (2015). The Phyre2 web portal for protein modeling, prediction and analysis. *Nature protocols* 10, 845-858.
- KYTE, J., AND DOOLITTLE, R.F. (1982). A simple method for displaying the hydropathic character of a protein. *Journal of molecular biology* 157, 105-132.
- LASKOWSKI, R.A., MACARTHUR, M.W., MOSS, D.S., AND THORNTON, J.M. (1993). PROCHECK: a program to check the stereochemical quality of protein structures. *Journal of applied crystallography* 26, 283-291.

- LÖWE, H., SCHMAUDER, L., HOBMEIER, K., KREMLING, A., AND PFLÜGER-GRAU, K. (2017). Metabolic engineering to expand the substrate spectrum of *Pseudomonas putida* toward sucrose. *Microbiologyopen* 6, e00473.
- MARTIN-PASCUAL, M., BATIANIS, C., BRUINSMA, L., ASIN-GARCIA, E., GARCIA-MORALES, L., WEUSTHUIS, R.A., VAN KRANENBURG, R., AND DOS SANTOS, V.A.M. (2021). A navigation guide of synthetic biology tools for *Pseudomonas putida*. *Biotechnology Advances* 49, 107732.
- MCGUFFIN, L.J., BRYSON, K., AND JONES, D.T. (2000). The PSIPRED protein structure prediction server. *Bioinformatics* 16, 404-405.
- PAUL, M., NAYAK, D.P., AND THATOI, H. (2020). Optimization of xylanase from *Pseudomonas mohnii* isolated from Simlipal Biosphere Reserve, Odisha, using response surface methodology. *Journal of Genetic Engineering and Biotechnology* 18, 1-19.
- ROY, A., YANG, J., AND ZHANG, Y. (2012). COFACTOR: an accurate comparative algorithm for structure-based protein function annotation. *Nucleic acids research* 40, W471-W477.
- SZKLARCZYK, D., GABLE, A.L., NASTOU, K.C., LYON, D., KIRSCH, R., PYYSALO, S., DONCHEVA, N.T., LEGEAY, M., FANG, T., AND BORK, P. (2021). The STRING database in 2021: customizable protein-protein networks, and functional characterization of user-uploaded gene/measurement sets. *Nucleic acids research* 49, D605-D612.
- TALAMANTES, D., BIABINI, N., DANG, H., ABDOUN, K., AND BERLEMONT, R. (2016). Natural diversity of cellulases, xylanases, and chitinases in bacteria. *Biotechnology for biofuels* 9, 1-11.
- TALENS-PERALES, D., SÁNCHEZ-TORRES, P., MARÍN-NAVARRO, J., AND POLAINA, J. (2020). *In silico* screening and experimental analysis of family GH11 xylanases for applications under conditions of alkaline pH and high temperature. *Biotechnology for biofuels* 13, 1-15.
- TERRAPON, N., LOMBARD, V., DRULA, E., COUTINHO, P.M., AND HENRISSAT, B. (2017). The CAZy database/the carbohydrate-active enzyme (CAZy) database: principles and usage guidelines. In *A practical guide to using glycomics databases* (Springer), pp. 117-131.
- TRAN, T.N., DOAN, C.T., AND WANG, S.-L. (2021). Conversion of wheat bran to xylanases and dye adsorbent by *Streptomyces thermocarboxydus*. *Polymers* 13, 287.
- VASIĆ, K., KNEZ, Ž., AND LEITGEB, M. (2021). Bioethanol production by enzymatic hydrolysis from different lignocellulosic sources. *Molecules* 26, 753.
- XU, D., AND ZHANG, Y. (2011). Improving the physical realism and structural accuracy of protein models by a two-step atomic-level energy minimization. *Biophysical journal* 101, 2525-2534.
- YU, C.S., CHEN, Y.C., LU, C.H., AND HWANG, J.K. (2006). Prediction of protein subcellular localization. *Proteins: Structure, Function, and Bioinformatics* 64, 643-651.